



Article

Satellite Monitoring of the Urban Expansion in the Pearl River–Xijiang Economic Belt and the Progress towards SDG11.3.1

Shuyue Liu ^{1,2}, Yan Yan ^{1,2,*} and Baoqing Hu ^{1,2}

¹ Key Laboratory of Environment Change and Resources Use in Beibu Gulf, Ministry of Education, Nanning Normal University, Nanning 530001, China; 200080604@email.nnnu.edu.cn (S.L.)

² Guangxi Key Laboratory of Earth Surface Process and Intelligent Simulation, Nanning 530001, China

* Correspondence: yanyan@nnnu.edu.cn

Abstract: Quantitative analysis of the spatiotemporal pattern of urban expansion and forecasting of the progress towards SDG11.3.1 are of great significance for the promotion of sustainable urban development. This study employed the spatiotemporal normalized threshold method to extract urban built-up areas in the Pearl River–Xijiang Economic Belt based on night-time light data and investigated the intricate patterns of urban expansion from 2000 to 2020. Then, the historical trends of the SDG11.3.1 indicators within the economic belt were evaluated, and future urban built-up areas were predicted based on the SSP1 scenario. The results indicate the following: (1) Built-up area extraction has an overall accuracy that exceeds 97% and G-mean values that all surpass 82%, indicating the high accuracy of the method. (2) The Pearl River–Xijiang Economic Belt demonstrates evident urban expansion trends, albeit with uneven development. The urban area of the economic belt has expanded from 1020.29 km² to 3826.87 km², the expansion direction of each city is different, and the center of gravity of the economic belt has moved to the southeast. (3) During the period from 2008 to 2020, the entire economic belt experienced a situation where the urban expansion rate was lower than the population growth rate, and there was an imbalance in urban development (LCRPGR = 0.33). However, looking ahead to the period from 2020 to 2030, the average LCRPGR for the entire economic belt shows a significant upward trend, approaching the ideal state of sustainable development (LCRPGR ≈ 1).

Keywords: urbanization; urban expansion; SDG11.3.1; night-time light data; Pearl River–Xijiang Economic Belt



Citation: Liu, S.; Yan, Y.; Hu, B. Satellite Monitoring of the Urban Expansion in the Pearl River–Xijiang Economic Belt and the Progress towards SDG11.3.1. *Remote Sens.* **2023**, *15*, 5209. <https://doi.org/10.3390/rs15215209>

Academic Editors: Qihao Weng, Hua Liu, Umamaheshwaran Rajasekar and Li Zhang

Received: 6 September 2023

Revised: 20 October 2023

Accepted: 28 October 2023

Published: 2 November 2023



Copyright: © 2023 by the authors. Licensee MDPI, Basel, Switzerland. This article is an open access article distributed under the terms and conditions of the Creative Commons Attribution (CC BY) license (<https://creativecommons.org/licenses/by/4.0/>).

1. Introduction

A rapid urbanization process has been occurring all over the world over the past several decades. The process is regularly accompanied by demographic growth and economic growth as well as the enlargement of urban land and the geographical spatial scope [1]. According to the world urbanization prospects reported by the United Nations, the urban population is expected to increase from about 56% in 2021 to 68% by 2050 [2]. The interdependence and mutual influence between urban expansion and population dynamics is changing. Urban sprawl and demographic growth have not only produced certain benefits but have also resulted in some problems such as environmental pollution [3], resource shortages [4], water stress, and so on [5]. Furthermore, urban expansion is a complex phenomenon involving diverse components [6]. As cities continue to expand, more rural populations are migrating to urban areas, thereby accelerating urban expansion. The actual growth in urban regions often does not match population growth, leading to an imbalance between the population and available land resources, resulting in inefficient land use and threatening the sustainability of urban development [7,8]. The intricate relationship between urban expansion and population dynamics changes is at the core of urban

sustainable development research. Therefore, a profound understanding of the synergies and trade-offs between urban expansion and population dynamics changes is crucial for devising effective strategies and guiding cities toward sustainable development [9].

At the United Nations Summit on Sustainable Development Goals, the declaration “Gearing up for a decade of action and delivery for sustainable development” was adopted. This marked the introduction of the SDGs (Sustainable Development Goals) as a comprehensive agenda aimed at addressing global challenges related to sustainable development. The SDGs are presented as a framework that comprises 17 distinct sustainable development goals, encompassing a total of 169 specific targets and 232 indicators. The primary purpose of this framework is to provide guidance for achieving sustainable development at various levels of society [10]. Owing to the importance of cities and human settlements, a specific goal, SDG11, is devoted to “sustainable cities and communities” [11] and the subordinate target 11.3 focuses on “inclusive and sustainable urbanization”. Specifically, the indicator SDG 11.3.1, defined as the ratio of the land consumption rate (LCR) to the population growth rate (PGR), can be utilized to measure urban land use efficiency in terms of urbanization sustainability [12]. As a result, it is essential to monitor these indicators, assess the relationships, and reveal the changes over time, as they contribute to targeted planning and guide cities toward sustainable urbanization. The accurate and timely quantification of urban expansion is crucial for the monitoring and evaluation of SDG 11.3.1. It also helps to predict progress toward the 2030 target of sustainable urbanization and the identification of potential gaps. Several studies have been conducted to quantify urban expansion and evaluate SDG 11.3.1. For example, Zhou et al. used Landsat images from the Google Earth Engine cloud platform to map built-up areas and analyze the urban scale and changes in morphology in the Beijing–Tianjin–Hebei region from 2000 to 2020, as well as the spatiotemporal dynamics of SDG 11.3.1 [13]. Wang et al. monitored land use efficiency indicators, including LCR, PGR, and LCRPGR, and depicted the spatial heterogeneity and dynamic trends of urban expansion and population growth in mainland China from 1990 to 2010 [7]. Gao et al. studied the Guangdong–Hong Kong–Macao Greater Bay Area in China, using LUCC remote sensing data along with comprehensive population and Gross Domestic Product data, and applied the Analytic Hierarchy Process to comprehensively assess the sustainable development level at the urban agglomeration and prefecture-level city scales for the periods of 2000–2010 and 2010–2020 [14]. It has been proven that the accurate quantification of urban expansion is crucial for assessing the progress of SDG 11.3.1 in order to better understand the sustainability of cities.

Nowadays, satellite remote sensing is recognized as one of the most effective tools for urban monitoring as it can provide continuous large-scale data at varying spatial and temporal resolutions. There have also been benefits from the development of remote sensing technologies combined with robust algorithms and high-performance computing systems [15,16]. The current state of research on urban built-up areas is generally extracted from two types of satellite remote-sensing images. One is land use and land cover data, which are usually generated from medium- or high-resolution remote sensing images, including Landsat series images and IKONOS, SPOT, and Quickbird data [17]. Due to the limited geographic coverage of such satellite images, considerable scenes are required to cover the regional or large scales. The pre-processing of raw data and the extraction of urban built-up areas are normally time-consuming, labor-intensive processes that require extensive specialized knowledge [18]. The utilization of cloud computing platforms and machine learning technologies in recent years has helped to improve the efficiency of identification and classification. However, it remains challenging to distinguish the bare background from the urban impervious surface due to the loose connection between human activities and the above-mentioned daytime satellite images [19]. The other is the utilization of night-time light satellite images for urban land interpretation. The ability to indicate the intensity of human habitation and activities allows the night-time light data to distinguish bright urban built-up land from the dim rural background [20]. There are two datasets that stand out as the primary sources of night-time light data in contemporary

studies. First, DMSP-OLS (Defense Meteorological Satellite Program Operational Line Scanner) is a satellite program that was launched by the United States Department of Defense with the primary purpose of monitoring night-time light conditions on Earth. It demonstrates the stable detection of lights from human settlements, especially in urban areas, making it suitable for monitoring the dynamic process of urban expansion at large spatial scales [18,21]. In DMSP night-time light imagery, a pronounced contrast is evident between illuminated urban regions and non-lit rural areas, enhancing the ease and precision when distinguishing between urban and rural land cover [22]. Second, NPP-VIIRS (National Polar-Orbiting Partnership–Visible Infrared Imaging Radiometer Suite) is a satellite system that was specifically crafted for Earth observations, which substantially improves the clarity and sensitivity of night-time light data [23]. NPP-VIIRS night-time light data are capable of collecting high-quality radiometric data. This is particularly well-suited for extracting urban land use information in areas with high rainfall, frequent cloud cover, or rapid urbanization [24]. The combination of two types of night-time light data allows for a comprehensive urban analysis, which takes into account the changes in urbanization patterns over different periods.

There are several popular methods to extract the urban built-up land from night-time light data, including the thresholding technique [25], Sobel-based edge detection [26], neighborhood statistics [27], and so on. Among these, the threshold method has been proven as a straightforward and robust method for urban land detection at the regional or national scales [28]. The thresholding method is simple and practical, with the threshold being adjustable according to the specific characteristics of the study area, offering flexibility in different scenarios. Integrating time series of DMSP-OLS and NPP-VIIRS night-time light data in urban studies offers the advantage of preserving the continuity of long-term research sequences [29]. To address the discrepancies in the spatial resolution, time series, etc., between DMSP-OLS and NPP-VIIRS night-time light data, the spatiotemporal heterogeneity of the two datasets is eliminated by using the Pseudo-Invariant Features method [22]. The core idea of the PIFs method is to establish a robust linear regression model to correlate the DN values of PIFs between the reference year and the target year and standardize the time series of continuous night-time light data. Subsequently, auxiliary information is utilized to determine the optimal threshold for each year in the entire time series of night-time light data.

Another noteworthy point is that previous studies on the implementation of SDGs have only focused on past progress and the current situation of SDGs, and some studies have also addressed the challenges faced at present and potential future opportunities [30,31]. However, there has been a lack of assessment regarding whether the sustainable urbanization goal will be achieved by the end of the implementation period for the SDGs in 2030 [32]. Therefore, it is an urgent priority to forecast the fulfillment of indicator 11.3.1, which is critical for policymakers to formulate long-term integrated strategies effectively. Predicting the expansion of urban land patterns is a relatively intricate process [33]. The forecasting of urban land patterns necessitates the development of predefined scenarios to represent potential future socioeconomic and environmental conditions [34]. It is necessary to develop scenarios that correspond to the future socioeconomic and environmental conditions of the specific regions. Shared Socioeconomic Pathways (SSPs) are a collection of scenarios used to describe potential future global socioeconomic and environmental developments. These scenarios are intended to assist researchers and policymakers in gaining a deeper comprehension of the various social, economic, and environmental development pathways. These also help to understand their potential impacts on climate change, sustainable development, and other global challenges [35]. The SSPs include SSP1 (sustainability), SSP2 (middle of the road), SSP3 (regional rivalry), SSP4 (inequality), and SSP5 (fossil-fuel development), representing distinct pathways. In this study, special emphasis is placed on the results of urban expansion under the SSP1 scenario. This choice is primarily because SSP1 represents a sustainable pathway that follows green development strategies [36], offering important new perspectives on potential sustainable urbanization trends for the future.

There are several ways to predict future urban land patterns, including cellular automaton [37–39], the artificial neural network [40–42], agent-based models [43–45], regression models [46–48], and so on. The logistic regression model can capture historical trends in urban area growth more accurately and can incorporate spatial variations in urbanization levels. This helps to obtain more reliable and scientifically rigorous predictions.

Therefore, our study aims to utilize a continuous time series of night-time light data to obtain urban built-up areas within the Pearl River–Xijiang Economic Belt. Additionally, we seek to conduct precise quantitative research on the spatiotemporal patterns of urban expansion in the economic belt’s urban agglomerations. Furthermore, we aim to assess and analyze the historical trends of the SDG11.3.1 indicator within the economic belt, along with forecasting the future urban built-up areas by utilizing the logistic regression model based on the SSP1 scenario. This comprehensive evaluation will enable us to assess the sustainable urbanization of the economic belt for the year 2030.

2. Materials and Methods

2.1. Study Area

The Pearl River–Xijiang Economic Belt is located between 104°29′E–114°04′E and 21°36′N–26°6′N, spanning across Guangdong province and Guangxi Zhuang autonomous region, uplinked to the provinces of Yunnan and Guizhou, and downlinked to Hong Kong and Macau. It encompasses 11 cities and 88 counties, serving as a crucial strategic region for China’s coordinated and sustainable development as well as its open cooperation with the Association of Southeast Asian Nations countries. The total area of the region is approximately 165,000 km², and the Yunnan–Guizhou Plateau, Guangxi Basin, Guangdong–Guangzhou Hills, and Pearl River Delta Plain are distributed in sequence from west to east [49]. The region is located in the tropical and subtropical monsoon climate zone and has a pleasant climate, distinct dry and wet seasons, and abundant precipitation.

By the end of 2020, the Pearl River–Xijiang Economic Belt had reached a total population of 62.57 million people with an urbanization rate of 71.09%. The region boasts excellent natural resources, favorable shipping conditions, a sound industrial foundation, promising prospects for cooperation, and tremendous development potential. Its expansion and development not only contribute to the fostering of new regional economic belts in China but also play a significant role in driving the development of the central–southern and southwestern regions. With the continuous expansion of the Pearl River–Xijiang Economic Belt, the rapid development of cities is increasing day by day. In the process of urbanization, it is particularly important to protect green spaces and reduce the negative impact on the environment to ensure alignment with sustainable development goals. The sustainability of cities is not only related to the quality of life of residents but also involves the broader ecological balance of the entire river basin. Therefore, it is necessary to carefully manage land resources, formulate eco-friendly urban policies, invest heavily in the construction of green infrastructure, and integrate it into the core considerations of development strategies. This is of great significance for strengthening the ecological construction and environmental protection of the entire river basin and promoting the sustainable development of the basin and cities [50] (Figure 1).

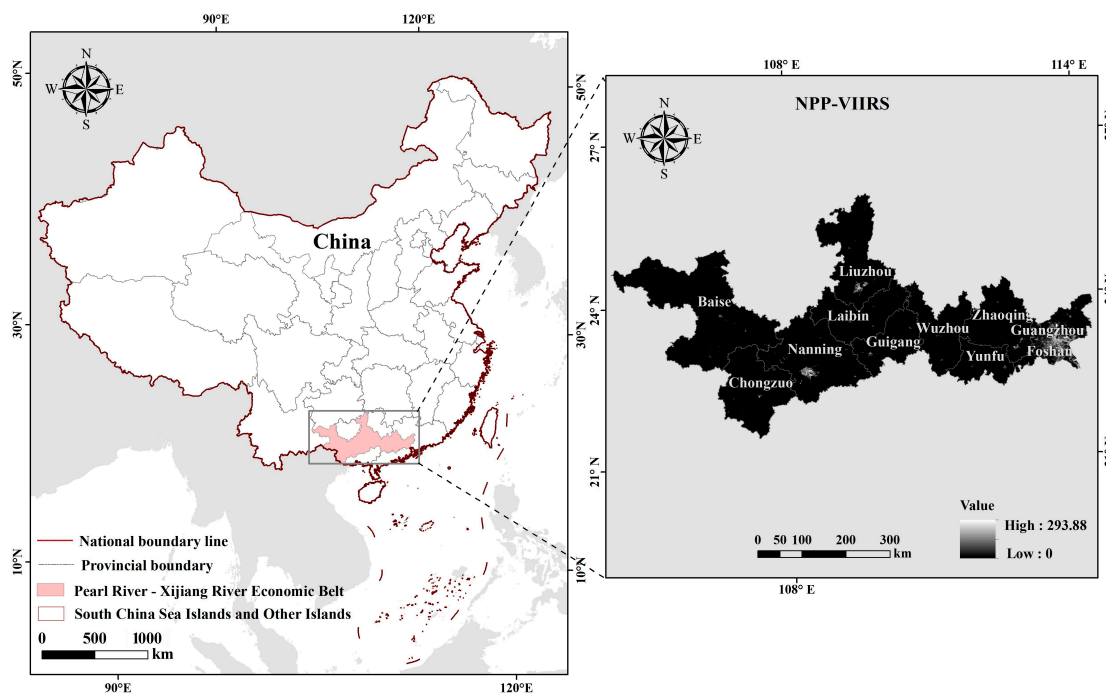


Figure 1. Location of the Pearl River–Xijiang Economic Belt.

2.2. Data Source

(1) DMSP-OLS night-time light data

The DMSP-OLS night-time light data were first released in 1992 and became the first global-scale satellite observation dataset of night-time light distribution. In this study, the stable night-time light data from 2000 to 2012, obtained from the fourth version of the DMSP-OLS annual data product developed by the National Geophysical Data Center (NGDC) of the National Oceanic and Atmospheric Administration (NOAA) in the United States, were utilized as the data source. The stable night-time light product was created by removing background noise and cleaning up transient light sources like wildfires, lightning, and fishing boats, making it suitable for studying global night-time light change trends and urbanization development [22].

(2) NPP-VIIRS night-time light data

The NPP-VIIRS_VNL V2 annual night-time light data from 2013 to 2020, developed in collaboration with NASA (National Aeronautics and Space Administration) and NOAA (National Oceanic and Atmospheric Administration) in the United States, were used as the data source. The NPP-VIIRS_VNL V2 data underwent a “Satellite–Ground Fusion” method during processing to remove the influence of unstable light sources, such as fires, and to enhance the quality and reliability of the data.

(3) Landsat remote sensing images

The high-resolution surface coverage information offered by Landsat remote sensing images allows for a comparison with brightness data from night-time light images, enabling the determination of thresholds between urban and non-urban areas. To determine the threshold between urban and non-urban regions using night-time light data and to further validate the accuracy of urban built-up area extraction results derived from night-time light data, this study employed Landsat remote sensing images from the years 2000, 2005, 2010, 2013, 2015, and 2020 as supplementary and validation datasets. The Landsat images were sourced from the United States Geological Survey (<https://earthexplorer.usgs.gov/>, accessed on 15 August 2022).

(4) Auxiliary Data

The high-resolution gridded China urban population forecast data (100 m) [51] and GDP forecast data [52] obtained from the Shared Socioeconomic Pathways (SSPs) were used and utilized as the basis for SSPs-consistent predictions. The statistical data were obtained from the “China Urban Construction Statistical Yearbook” and the “China City Statistical Yearbook” for the years 2001 to 2021, as well as “China Population and Employment Statistical Yearbook”, “Guangdong Statistical Yearbook”, “Guangzhou Statistical Yearbook”, and “Guangxi Statistical Yearbook”. The key indicators included the built-up area, urban resident population, total population within the urban district, and annual GDP.

The geospatial data used in this study are detailed in Table 1.

Table 1. Data Sources and Descriptions.

Data Sets	Resolution	Timespan	Source
DMSP-OLS night-time light data	1 km	2000–2012	NOAA/NGDC (https://ngdc.noaa.gov/eog/download.html , accessed on 15 August 2022)
NPP-VIIRS night-time light data	500 m	2013–2020	NOAA/NGDC (https://ngdc.noaa.gov/eog/download.html , accessed on 15 August 2022)
Landsat remote sensing data	30 m	2000–2020	USGS (https://earthexplorer.usgs.gov/ , accessed on 15 August 2022)
Mainland China SSP population grids	100 m	2020–2030	Chen et al. (2020) [51].
Global SSP GDP grids	1 km	2020–2030	Wang et al. (2022) [52].

2.3. Methods

Pseudo-Invariant Features (PIFs) refer to urban areas, typically mature neighborhoods, where the intensity of night-time light emissions remains relatively constant over a certain period of time. These urban features are termed “pseudo-invariant” because their night-time light intensity experiences minimal variation over time [22,53]. This study refers to the normalized threshold method based on the concept of Pseudo-Invariant Features (PIFs) proposed by Wei et al. [22] and Xie et al. [54], which was applied to both DMSP-OLS and NPP-VIIRS night-time light data to derive results. This approach allows for the determination of optimal thresholds for each city, enabling the accurate delineation of built-up and non-built-up areas and obtaining critical information on urban expansion. Based on the extracted urban built-up areas, the spatial and temporal patterns of urban expansion in the economic belt were analyzed. Then, the overall performance of the implementation of SDG11.3.1 and the gap to the 2030 target were evaluated based on SSP1 scenarios (Figure 2).

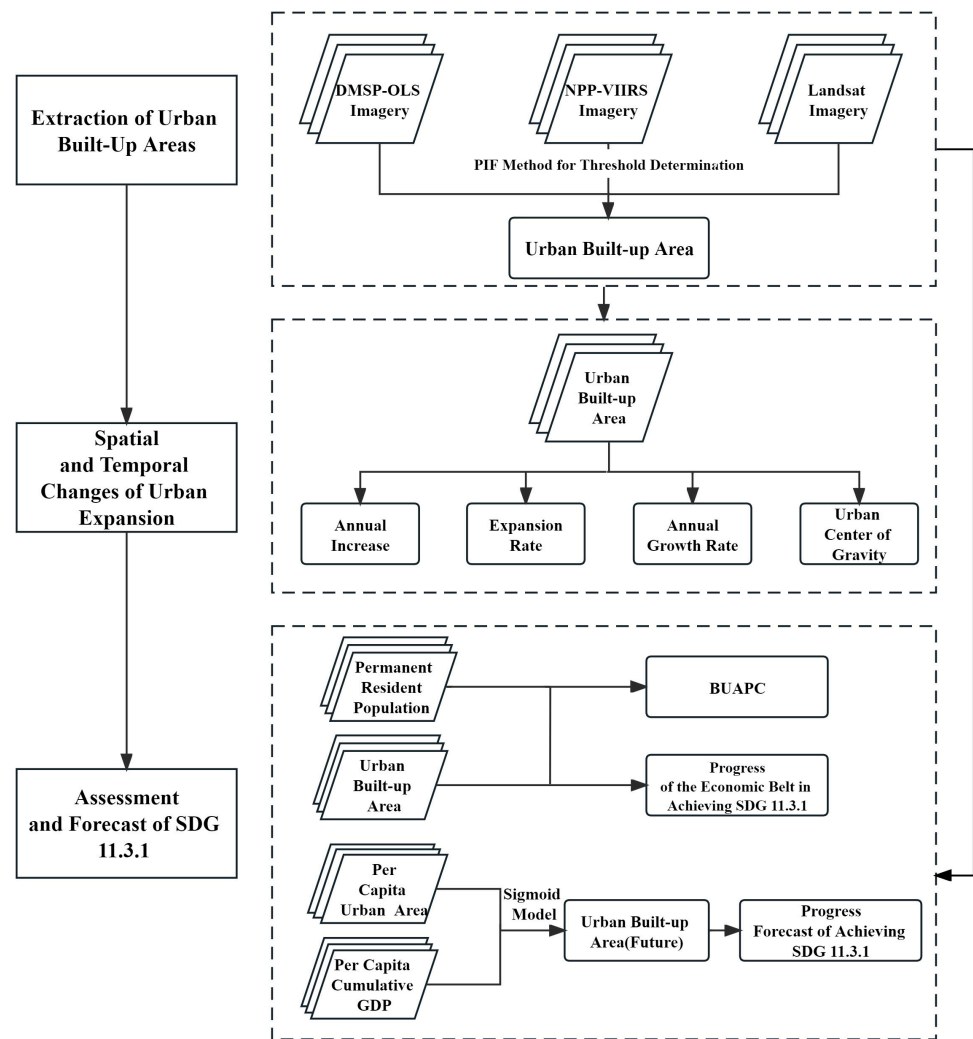


Figure 2. Workflow of the study.

2.3.1. PIFs Method for Threshold Determination

The PIFs method relies on the irreversibility of urbanization processes and references high-resolution Landsat remote sensing imagery to screen PIFs within the night-time light data from the baseline year. The optimal thresholds for each year's urban built-up area are determined based on the reference threshold from the baseline year, thus enabling the extraction of the urban area [55]. In this study, considering the difference in the temporal coverage of the two night-time light datasets, 2000 and 2013 were selected as the respective baseline years for each dataset. The method's details are as follows:

First, all remote sensing data were preprocessed using ArcGIS 10.3, including image mosaicking, cropping, and reprojection. Then, by visually interpreting the Landsat remote sensing images of the baseline year, built-up areas for the 11 cities of the study area were identified and calculated. A comparison analysis was conducted between the built-up areas calculated from Landsat remote sensing images and those extracted from the night-time light data of the baseline year. By applying the binary iterative method in Equation (1), the potential threshold was incrementally increased from 1 by iteratively testing different potential thresholds for partitioning the night-time light data into built-up and non-built-up areas. Until the error (DN_t) reaches its minimum value, the potential threshold at this point equals the optimal reference threshold. Hence, the optimal reference threshold for each city can be determined using the night-time light data from the base year [56]. The

correlation coefficient of the total built-up area within the economic belt obtained from the two datasets reached 0.998.

$$\text{Error} (DN_t) = S_{\text{NTL}} - S_{\text{Landsat}} \quad (1)$$

where DN_t represents the potential threshold, and S_{NTL} and S_{Landsat} denote the built-up areas extracted from night-time light data and calculated from Landsat remote sensing images, respectively.

Next, the PIFs regions for the baseline year and target year were identified, ensuring that the DN values within the PIFs regions were less than 59. By employing a linear regression model based on Equation (2), relationships were established between the DN values of the baseline year and those of the target year.

$$\text{PIFs}_t = \alpha \times \text{PIFs}_0 + \beta \quad (2)$$

where α and β represent the regression coefficients, PIFs_0 denotes the DN value of the PIFs region in the baseline year, and PIFs_t represents the DN value of the PIFs region of the same pixel in year t .

Based on Equation (1), the optimal reference threshold for extracting urban built-up areas was derived, and then Equation (3) was combined to predict the optimal threshold for extracting urban built-up areas in year t .

$$\text{Thresholds}_t = a \times \text{Thresholds}_0 + b \quad (3)$$

where a and b represent the regression coefficients. Thresholds_0 and Thresholds_t represent the optimal reference threshold in the baseline year and the optimal threshold for urban built-up areas in the target year, respectively.

Finally, the extracted results were verified and corrected to generate more accurate urban built-up areas.

2.3.2. Validation and Accuracy Assessment

The Overall Accuracy (OA), which represents the proportion of correctly classified pixels compared to the total number of pixels in the image, is one of the critical indicators used to measure the accuracy of the classification results.

The G-mean not only considers the number of correctly classified pixels but also takes into account the number of misclassified pixels. In the case of an imbalanced class distribution, G-mean provides a better assessment of the spatial accuracy of the classification results, offering more comprehensive and accurate information [22,54,57]. The equation for calculating the G-mean is as follows:

$$\text{G-mean} = \sqrt{\frac{d}{b+d} \times \frac{d}{c+d}} \quad (4)$$

where d represents the number of correctly classified urban pixels, and b and c represent, respectively, the numbers of urban and non-urban pixels that do not match the actual classification in the classification results based on night-time light data and Landsat remote sensing images.

2.3.3. Urban Expansion Indicators

To better observe the changing trends for urban built-up areas during different time periods, the time span from 2000 to 2020 was divided into four consecutive sub-periods: 2000–2005, 2005–2010, 2010–2015, and 2015–2020.

Three indicators were employed to explore the temporal variation characteristics of urban built-up areas, i.e., the Annual Increase (AI), Expansion Rate (ER), and Annual Growth Rate (AGR) [20,58,59]. The AI reflects the trend in the changes in urban built-up areas over time. The ER can be used to measure how fast a city is expanding over a

specific period, while the AGR allows for a comparison of the urban expansion in different city clusters by eliminating the influence of the city size. The combined analysis of these indicators provides a comprehensive assessment of the scale, speed, and intensity of urban expansion within the economic belt, offering a scientific basis for sustainable urban development. The calculation methods are illustrated in Equations (5)–(7).

$$AI = \frac{UA_{(n+i)} - UA_i}{n} \quad (5)$$

$$ER = \frac{UA_{(n+i)} - UA_i}{n \times UA_i} \times 100\% \quad (6)$$

$$AGR = \left[\left(\frac{UA_{(n+i)}}{UA_i} \right)^{\frac{1}{n}} \right] - 1 \times 100\% \quad (7)$$

where AI represents the Annual Increase, ER stands for the Expansion Rate, and AGR denotes the Annual Growth Rate. UA_i represents the urban built-up area in year i , while $UA_{(n+i)}$ represents the urban built-up area in year $n + i$, and n is the time interval.

The spatial patterns and variation in the urban built-up area were analyzed by the Standard Deviation Ellipse (SDE) indicator. The SDE is a tool that uses statistical methods to analyze the spatial distribution characteristics of geographic elements. It can be utilized to determine the expansion direction and range of urban built-up areas. The long axis of the ellipse represents the main distribution direction of urban built-up areas, while the short axis represents the distribution range, and the center of the ellipse represents the center of urban built-up areas. The SDE, the migration angle, and the migration rate were calculated by Equations (8)–(11):

$$SDE_x = \sqrt{\frac{\sum_{i=1}^n (x_i - \bar{X})^2}{n}} \quad (8)$$

$$SDE_y = \sqrt{\frac{\sum_{i=1}^n (y_i - \bar{Y})^2}{n}} \quad (9)$$

where x_i and y_i represent the spatial coordinates of each city center, while X and Y represent the arithmetic mean center.

$$\theta = \tan^{-1} \frac{|Y_{t+1} - Y_t|}{|X_{t+1} - X_t|} \times 180^\circ / \pi \quad (10)$$

where θ represents the migration angle of the center of gravity of the urban area, X_{t+1} , and Y_{t+1} represent the coordinates of the urban center at the end of the study period, and X_t and Y_t represent the coordinates of the urban center at the beginning of the study period.

$$V = \frac{\sqrt{(X_{t+1} - X_t)^2 + (Y_{t+1} - Y_t)^2}}{T_{t+1} - T_t} \quad (11)$$

where V represents the migration rate of the urban center of gravity, and T_{t+1} and T_t represent the end period and the beginning period of the study period, respectively.

2.3.4. Assessment and Forecast of SDG 11.3.1

Based on the characteristics of the study area, we localized the SDG 11.3.1 indicator to better analyze the changing trends of the indicator by regularly monitoring it every five years. Since the official statistics of each city do not provide the permanent residents' data

for the municipal districts before 2008, this study used the data on permanent residents (within the city proper) produced since 2008 and the previously obtained urban built-up area extraction results for the SDG 11.3.1 assessment. Such a selection takes into account the principles of reliability of assessment, consistency, and availability and comparability of data. The LCR and PGR quantitatively describe the expansion intensity and demographic changes in two phases. The equation for calculating the LCR and PGR is as follows [7,60]:

$$\text{LCRPGR} = \frac{\text{LCR}}{\text{PGR}} = \frac{\ln(\text{Urb}_{n+i}/\text{Urb}_i)/n}{\ln(\text{Pop}_{n+i}/\text{Pop}_i)/n} \quad (12)$$

where the LCR typically refers to the increment in the urban built-up area per unit of time, while the PGR represents the rate of population increase over a specific period. Urb_{n+i} and Urb_i denote the urban built-up area at the end and beginning of the study period, respectively, and Pop_{n+i} and Pop_i represent the permanent resident population at the end and beginning of the study period, with n representing the number of years between the two periods.

When the LCRPGR is less than 0, it can be divided into two cases. In the case where $\text{LCRPGR} < -1$, when the LCR is positive and the PGR is negative, inefficient land use is indicated, where the population growth rate is lower than the land consumption rate. When the LCR is negative and the PGR is positive, inefficient land use is indicated, with the land consumption rate being lower than the population growth rate, resulting in insufficient land per capita. In the case of $-1 < \text{LCRPGR} < 0$, when the LCR is positive and the PGR is negative, a move away from efficiency is suggested, as the population growth rate is lower than the land consumption rate. When the LCR is negative and the PGR is positive, a move away from efficiency is suggested, as the land consumption rate is lower than the population growth rate, leading to insufficient land per capita.

When the LCRPGR is greater than 0, it can be divided into two cases. In the case of $0 < \text{LCRPGR} < 1$, when both the LCR and PGR are positive, a move toward efficiency is indicated, there is population growth, and the increase in the built-up area is developing in a balanced direction. When both the LCR and PGR are negative, a move toward efficiency is indicated, there is a population decrease, and the reduction in built-up area is developing in a balanced direction. In the case of $\text{LCRPGR} > 1$, when both the LCR and PGR are positive, a move away from efficiency is indicated, where the population growth rate is lower than the land consumption rate. When both the LCR and PGR are negative, a move away from efficiency is suggested, where the land consumption rate is lower than the population growth rate [61].

Ideally, the LCRPGR should be approximately equal to 1, with the LCR and PGR developing in synchrony, indicating that the city's land expansion and population growth are in harmony.

To comprehensively assess the urbanization sustainability within the economic belt, the introduction of the Built-Up Area Per Capita (BUAPC) helps to explain the value of the main indicator, LCRPGR, and can better reveal the sustainability characteristics of the urbanization process within the economic belt. The calculation equation for the BUAPC is as follows:

$$\text{BUAPC} = \frac{\text{Urb}_t}{\text{Pop}_t} \quad (13)$$

where Urb_t represents the urban built-up area in year t , and Pop_t represents the permanent resident population (within the city proper) in year t .

We built a predictive model for urban built-up areas in the study region using Python programming language and conducted scenario simulations based on the sustainable development path of SSPs. By generating annual predictions of urban built-up areas consistent with the SSP1 scenario, the future urbanization sustainability of the study area up to the year 2030 was assessed according to SDG 11.3.1.

A sigmoid model using the permanent resident population data for each city starting from the year 2000 was employed, and using previously obtained urban built-up area

extraction results, the per capita cumulative GDP (in yuan) of each city was integrated to predict the expansion of each city within the economic belt. The aims were to capture the historical trends in urban area growth more accurately and to incorporate spatial differences in urbanization levels to allow more reliable and scientifically rigorous predictions. The calculation used is as follows:

$$pBUA_t = a + \frac{b}{1 + \exp^{-c \times (pCumGDP_t - d)}} \quad (14)$$

where $pBUA_t$ and $pCumGDP_t$ represent the natural logarithm of the per capita urban built-up area and per capita cumulative GDP in year t , respectively. The parameters a and b represent the heterogeneity of the urbanization process in each city, while c and d represent coefficients that collectively determine the shape of the sigmoid growth curve for built-up areas [62,63]. Since the cumulative GDP considers the economic performance of the study area over multiple years, it is more stable and better aligns with long-term sustainability concerns for economic growth compared to the annual GDP. Therefore, the study uses the per capita cumulative GDP to predict urban expansion. The parameters a , b , c , and d were fitted using the Maximum Likelihood Estimation (MLE) method, and subsequently, the per capita urban built-up area was obtained for each city under the SSP1 scenario.

$$BUA_t = pBUA_t \times P_t \quad (15)$$

where BUA_t and P_t represent the urban built-up area and predicted population data for year t under the SSP1 scenario, respectively.

3. Results

3.1. Accuracy Validation

By comparing the built-up areas obtained from the optimal thresholds predicted based on night-time light data with those derived from the optimal thresholds of the Landsat remote sensing imagery, the accuracy validation results were obtained for each city for four periods (Figure 3).

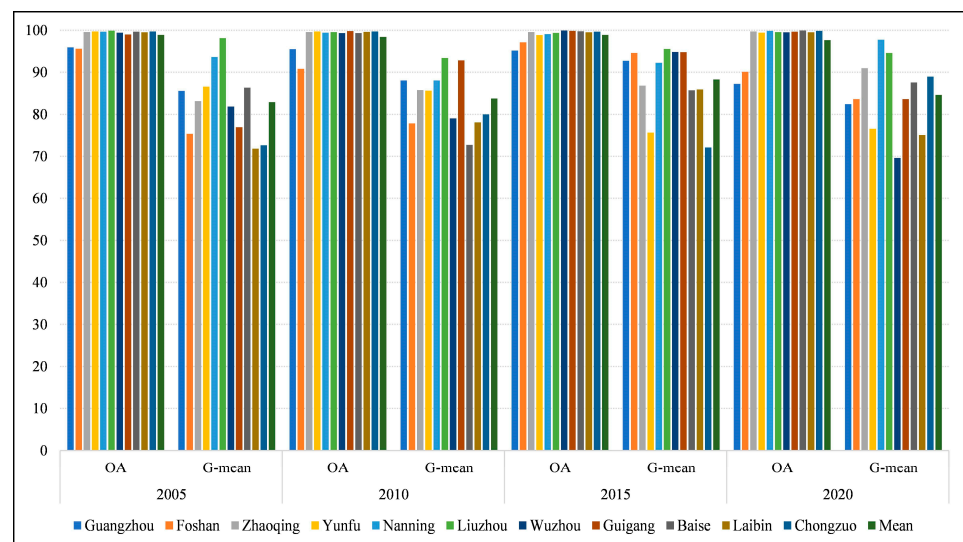


Figure 3. Accuracy validation of urban built-up areas (%).

The OA values of the urban built-up area extraction for the four validation years all exceeded 87%, with all average values exceeding 97%. Additionally, except for the G-mean value for Wuzhou City in 2020, which was 69.63%, the G-mean values for the other years of other cities all exceeded 70%, and all average G-mean values exceeded 82%. The validation

results indicated that the extraction results were reliable and could meet the requirements for subsequent studies.

3.2. Spatial and Temporal Changes in Urban Expansion

3.2.1. Spatial Pattern and Changes in the Urban Built-Up Area

The overall development trend of the entire Pearl River–Xijiang Economic Belt has been consistent, but the expansion and development of individual cities have been uneven (Figure 4). The Guangzhou city of Guangdong province has undergone rapid growth and expansion at a visible speed, which has also driven the development of surrounding cities, especially those with increasingly close connections to Foshan city. Accordingly, rapid growth has been observed in the capital city (Nanning city) and industrial city (Liuzhou city) of the Guangxi Zhuang autonomous region. The other cities in the two administrative regions were not that obvious, which indicates the varying urban built-up area expansion trends among the cities of the Pearl River–Xijiang Economic Belt.

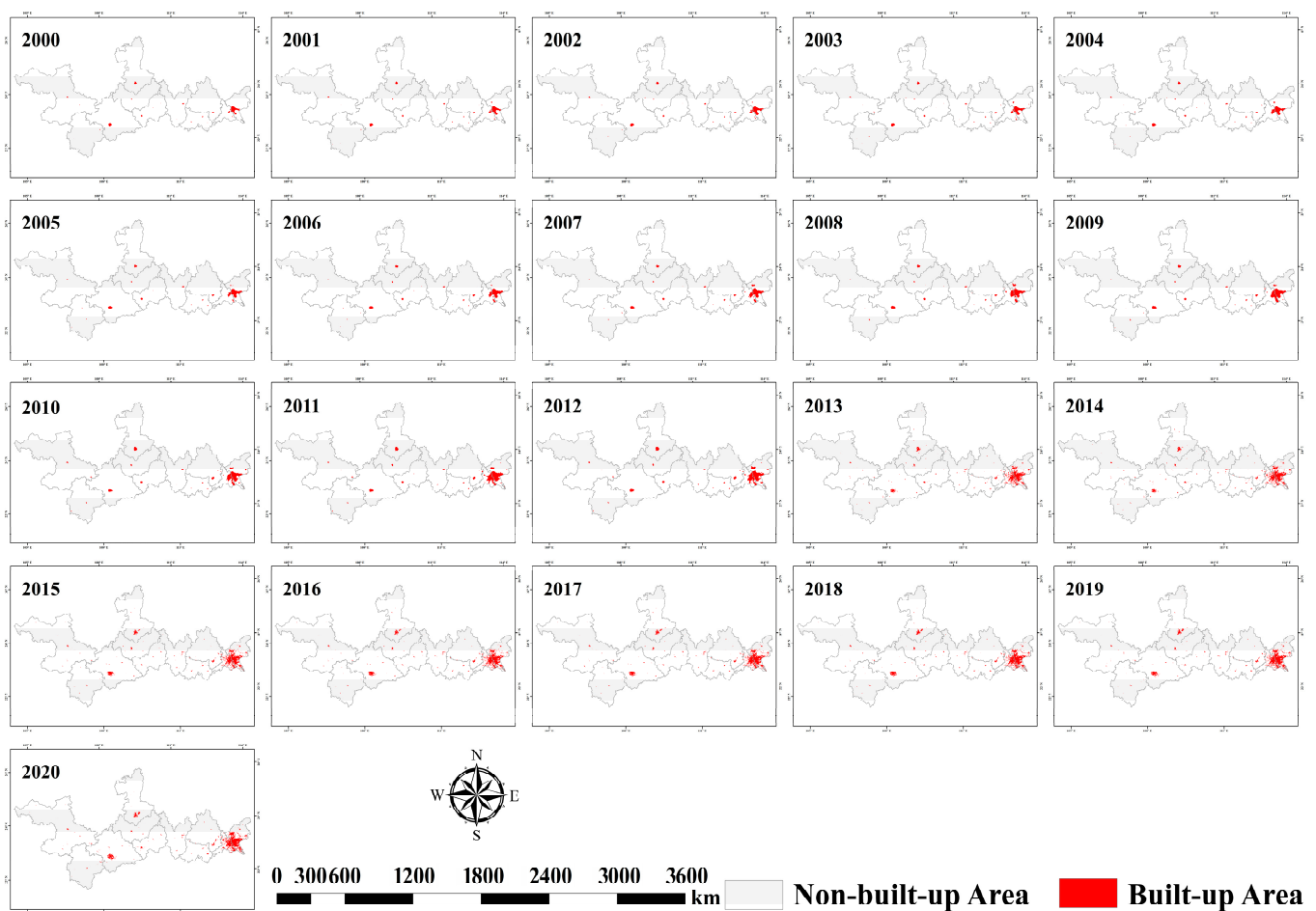


Figure 4. Spatial Pattern of Urban Built-up Areas from 2000 to 2020.

From 2000 to 2020, the spatial-temporal pattern of cities across the entire Pearl River–Xijiang Economic Belt showed a clear trend of expansion (Figure 5). For the Pearl River–Xijiang Economic Belt, the urban built-up area has been expanding year by year. Guangzhou and Foshan, as vital central cities within the economic belt, have undergone rapid development and urbanization processes. The urban expansion of Guangzhou and Foshan demonstrates a radiating pattern with the city center as the core, extending gradually towards the surrounding areas. This implies that urban construction activities are primarily concentrated in the periphery of the existing city center, progressively extending towards the urban fringe areas.

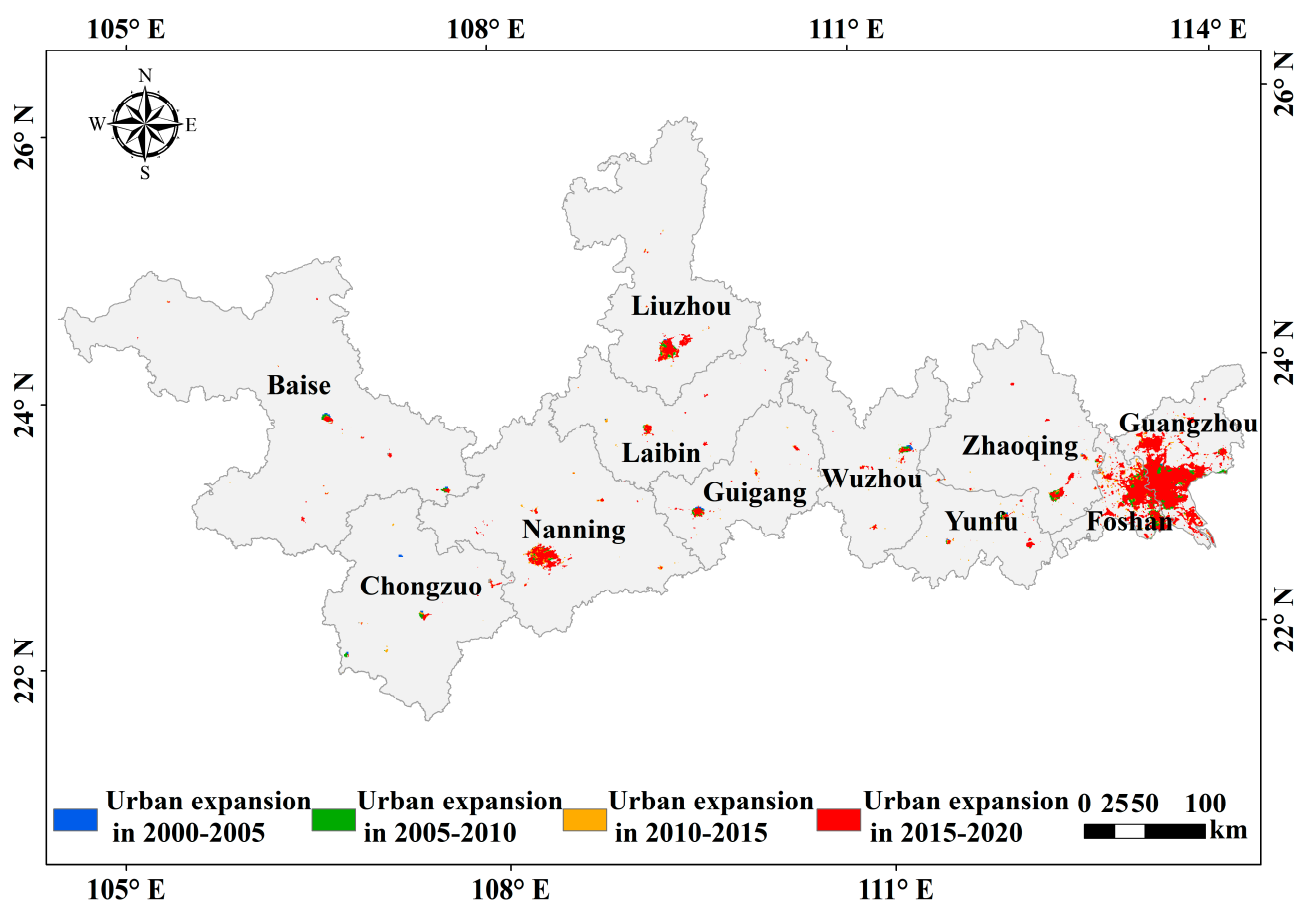


Figure 5. Spatial pattern of urban expansion in the Pearl River–Xijiang Economic Belt from 2000 to 2020.

3.2.2. Temporal Variation of Urban Expansion

The urban built-up areas of the Pearl River–Xijiang Economic Belt increased from 1020.29 km² to 3826.87 km² from 2000 to 2020. Compared to 2000, the built-up area of the whole study area increased by approximately 275.08% in 2020. Guangzhou experienced the greatest increment in the built-up area and increased by 1270.54 km² during this period. This was followed by Foshan, Nanning, and Liuzhou, which increased by 891.41 km², 206.15 km², and 123.68 km², respectively. The increases in the urban built-up areas were all below 100 km² for the remaining cities.

In the past two decades, the Annual Increase (AI), Urban Expansion Rate (ER), and Annual Growth Rate (AGR) of the Pearl River–Xijiang Economic Belt were 140.33 km², 13.75%, and 6.83%, respectively (Table 2). Guangzhou and Foshan have both experienced significant urban expansion over the past 20 years. Specifically, the AI values for Guangzhou and Foshan were 63.53 km² and 44.57 km², respectively, which are much higher than those of other cities. The ER of Foshan was the best with 58.38%, and Foshan also had the highest AGR, which was 13.54%. It is worth mentioning that Chongzuo and Laibin ranked second and third for both the ER and AGR indicators, revealing a notable trend for built-up area growth.

Table 2. Annual Increase (AI, km²), Expansion Rate (ER, %), and Annual Growth Rate (AGR, %) in the Pearl River–Xijiang Economic Belt from 2000 to 2020.

		Guangzhou	Foshan	Zhaoqing	Yunfu	Nanning	Liuzhou	Wuzhou	Guigang	Baise	Laibin	Chongzuo	Economic Belt
AI	2000–2005	49.14	35.24	2.97	1.35	7.13	3.65	1.39	2.97	1.98	1.88	1.58	109.30
	2005–2010	70.38	76.33	5.61	1.75	10.25	6.24	1.16	0.74	2.26	2.05	2.21	178.98
	2010–2015	84.55	47.07	5.65	3.11	17.79	7.58	2.83	3.28	2.19	4.19	1.64	179.88
	2015–2020	50.03	19.64	2.87	0.95	6.06	7.26	1.73	1.12	1.92	0.83	0.74	93.16
	2000–2020	63.53	44.57	4.28	1.79	10.31	6.18	1.78	2.03	2.09	2.24	1.54	140.33
ER	2000–2005	8.81	46.16	6.64	5.49	6.14	3.77	5.10	8.95	8.03	17.45	19.74	10.71
	2005–2010	8.76	30.22	9.40	5.59	6.75	5.43	3.38	1.54	6.52	10.16	13.91	11.42
	2010–2015	7.32	7.42	6.44	7.75	8.76	5.18	7.05	6.33	4.78	13.80	6.07	7.31
	2015–2020	3.17	2.26	2.48	1.72	2.08	3.94	3.19	1.64	3.39	1.61	2.10	2.77
	2000–2020	11.39	58.38	9.54	7.29	8.88	6.39	6.51	6.10	8.47	20.78	19.26	13.75
AGR	2000–2005	7.57	27.03	5.90	4.97	5.50	3.51	4.64	7.68	6.99	13.37	14.72	8.96
	2005–2010	7.54	20.00	8.01	5.05	5.99	4.92	3.18	1.49	5.81	8.56	11.14	9.46
	2010–2015	6.44	6.52	5.74	6.77	7.54	4.72	6.23	5.66	4.38	11.07	5.45	6.43
	2015–2020	2.99	2.16	2.36	1.66	2.00	3.66	3.00	1.59	3.18	1.56	2.01	2.63
	2000–2020	6.12	13.54	5.48	4.60	5.24	4.20	4.26	4.07	5.08	8.55	8.22	6.83

Note: Different time periods represent different study periods, i.e., “2000–2005” represents the time span from 2000 to 2005, and so forth.

The maximum values of AI occurred during the period from 2010 to 2015 for most cities, except for Foshan, Chongzuo, and Baise. The three indicators (AI, ER, and AGR) dropped at visible speed from 2015 to 2020 compared to the previous periods for all cities.

3.2.3. Urban Built-Up Area Center Migration

The urban center of the Pearl River–Xijiang Economic Belt is located at (110.977°E–112.25°E, 23.334°N–23.202°N). The weighted standard deviation ellipses of the study area gradually shifted toward the eastern direction, and the center shifted by 129.83 km (Table 3).

Table 3. Migration angle (°), migration rate (km/a), and migration distance (km) in the Pearl River–Xijiang Economic Belt from 2000 to 2020.

	Migration Angle	Migration Rate	Migration Distance
2000–2005	26.57	0.09	0.46
2005–2010	3.64	9.39	46.94
2010–2015	3.12	15.52	77.58
2015–2020	7.02	1.16	5.80
2000–2020	2.96	6.49	129.83

The migration distance of the economic belt’s center was very small from 2000 to 2005. Subsequently, the migration distance increased and reached a maximum of 77.58 from 2010 to 2015. However, the migration distance dropped sharply in the period of 2015 to 2020, which corresponds with the spatial and temporal variation in the urban built-up area.

The centroid of the economic belt in 2005 (110.983°E, 23.32°N) migrated at an average annual speed of 9.39 km/a in the southeast direction with a shift of 3.64° and moved to the center of the economic belt in 2010 (111.431°E, 23.307°N). This indicates that the growth center of the built-up area shifted southeast during this period. From 2015 to 2020, the urban center migrated at an average annual speed of 1.16 km/a in the southeast direction with a shift of 7.02°.

The centers of gravity of Baise City and Yunfu City both moved to the southeast, which was the same direction as the entire economic belt (Figure 6). Guangzhou, Zhaoqing, Nanning, Liuzhou, Guigang, and Laibin showed a clear trend of expansion in the northeast direction. The center migration directions of Foshan, Wuzhou, and Chongzuo were towards the southwest.

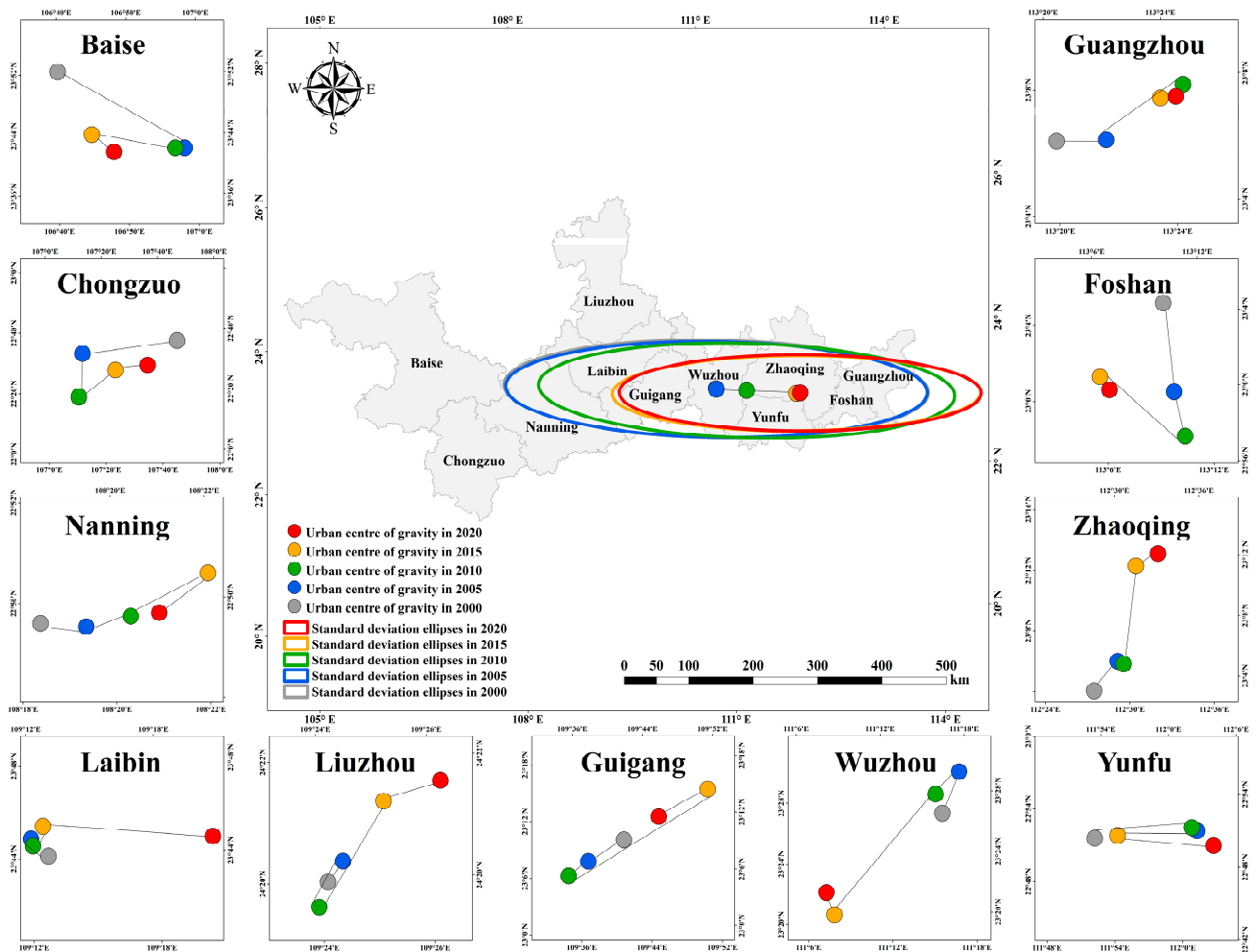


Figure 6. Direction and trajectory changes of urban centroid migration in the Pearl River–Xijiang Economic Belt from 2000 to 2020.

3.3. Urbanization Sustainability of the Economic Belt

3.3.1. Progress of the Economic Belt in Achieving SDG 11.3.1

During the period of 2008 to 2020, the average LCRPGR for the entire economic belt was 0.33. This signifies that, during this period, urban expansion and population growth in the economic belt were both moving in a balanced and efficient direction. The LCRPGR values were positive in most cities except Laibin (Figure 7d). The negative LCRPGR value for Laibin was due to its negative PGR, indicating a decrease in the resident population from 2008 to 2020, resulting in a mismatch between urban expansion and population growth. Among the cities with positive LCRPGR values, Guigang had the highest LCRPGR (5.9), indicating that its land consumption rate surpassed the population growth rate from 2008 to 2020. Next, were Wuzhou (1.94), Chongzuo (1.65), and Foshan (1.07). The LCRPGR of the remaining cities was between 0 and 1, which means that these cities are moving towards efficient land use.

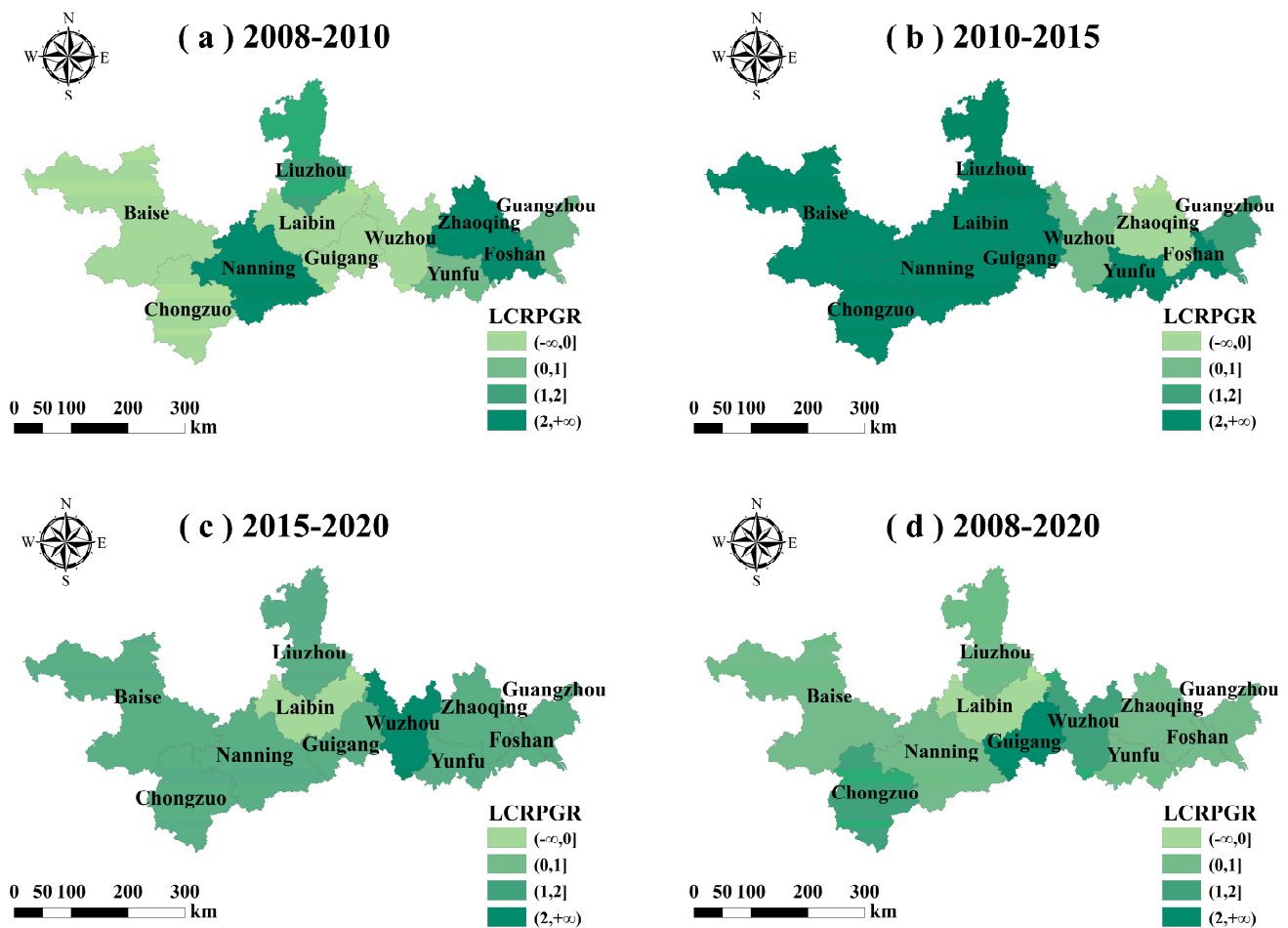


Figure 7. Spatial changes in the land Consumption Rate per Population Growth Rate (LCRPGR) in the Pearl River–Xijiang Economic Belt from 2008 to 2020.

From 2008 to 2010, Zhaoqing had the highest LCRPGR (14.78), followed by Foshan (2.47), Nanning (2.19), and Liuzhou (1.10) (Figure 7a). From 2010 to 2015, the LCRPGR of most cities presented an increasing trend and reached their peaks except Zhaoqing (Figure 7b). The decrease in the LCRPGR of Zhaoqing can be attributed to its significant population growth, which was one of the main reasons for the decline. From 2015 to 2020, most cities had positive LCRPGR values, except for Laibin with an LCRPGR of -2.60 (Figure 7c).

Generally, the LCRPG of the entire Pearl River–Xijiang Economic Belt showed an initial upward trend followed by a subsequent decline. During the period from 2015 to 2020, the LCRPGR gradually declined to 0.29, indicating that the urban expansion speed in the economic belt has gradually slowed down, because the urban development has gradually entered a relatively stable stage, and the supply of land resources is relatively stable.

Most cities showed an upward trend in the per capita built-up area (BUAPC), especially Foshan and Laibin, which aligns with the significant urban expansion in Foshan and the decrease in the permanent resident population in Laibin. Compared to 2008, Guangzhou, Zhaoqing, Yunfu, and Nanning experienced a gradual decline in the BUAPC by 2020. This indicates a relatively slower expansion rate compared to population growth (Figure 8).

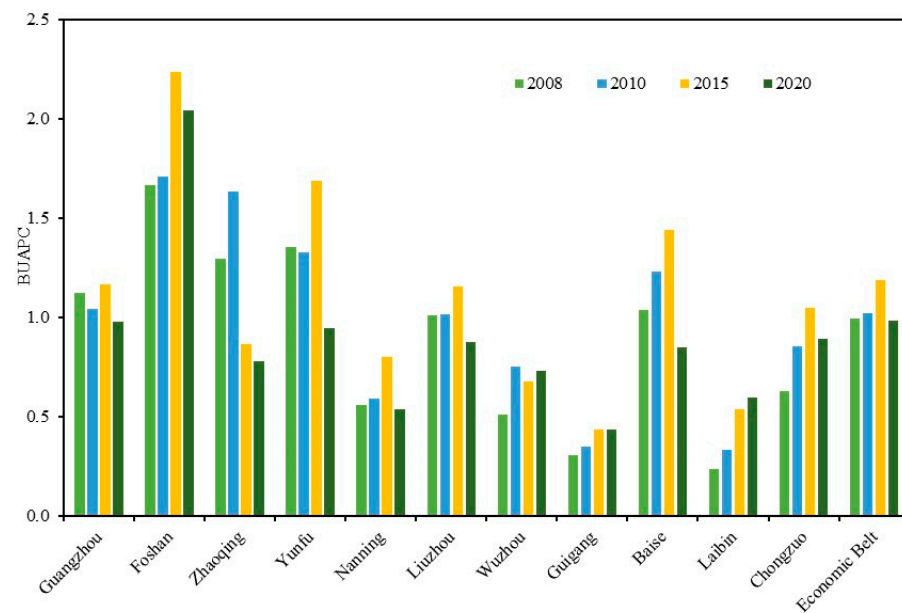


Figure 8. Changes in the per capita built-up area (BUAPC) in the Pearl River–Xijiang Economic Belt from 2008 to 2020.

3.3.2. Progress of the Economic Belt in Achieving SDG 11.3.1

The prediction results were validated by comparing the extracted urban built-up area in 2020 from previous night-time light data with the projected urban built-up area under the SSP1 scenario (Figure 9). The validation results obtained from comparing the model predictions with the previous extraction results indicate an R^2 value greater than 0.9, signifying good fitness between the model predictions and the actual extraction results. This demonstrates that the model performs well and exhibits high accuracy when predicting urban area growth. Thus, the urban built-up area of the sigmoid model projection under the SSP1 scenario can be utilized to calculate the LCRPGR indicator to assess the level of urbanization sustainability in economic belt development by the year 2030.

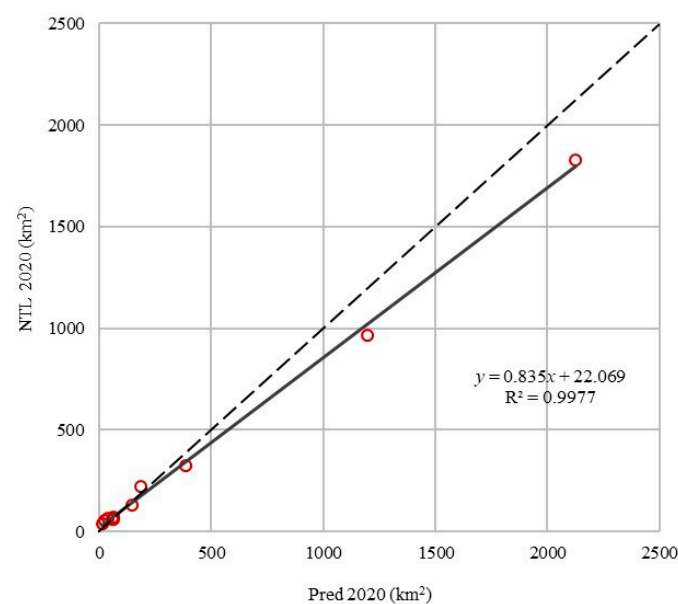


Figure 9. Comparison between sigmoid model predictions and night-time light data extraction results.

Table 4 illustrates the variation in the LCRPGR within the Pearl River–Xijiang Economic Belt during the period from 2020 to 2030, aiding in the assessment of whether the economic belt can achieve the objectives set by SDG11.3.1 by 2030. Throughout the years 2020 to 2030, the average LCRPGR for the entire economic belt exhibited an increasing trend, approaching the ideal state (LCRPGR \approx 1) by 2030. From 2020 to 2025, the LCRPGR values of Guangzhou, Foshan, Laibin, and Chongzuo nearly reached the ideal state. Meanwhile, the LCRPGR values of Yunfu (1.26), Liuzhou (1.31), and Guigang (1.11) were higher than the economic belt’s average (0.88), while the LCRPGR values of the rest of the cities ranged between 0 and 1. From 2025 to 2030, the LCRPGR values for all cities approached 1, indicating significant progress in terms of urbanization sustainability for the entire economic belt.

Table 4. Changes in the LCRPGR in the Pearl River–Xijiang Economic Belt from 2020 to 2030.

	LCRPGR	
	2020–2025	2025–2030
Guangzhou	1.00	1.00
Foshan	1.00	1.00
Zhaoqing	0.31	1.00
Yunfu	1.26	1.00
Nanning	0.25	1.00
Liuzhou	1.31	1.00
Wuzhou	0.87	1.00
Guigang	1.11	1.00
Baise	1.00	1.00
Laibin	0.56	1.00
Chongzuo	1.00	1.00
Economic Belt Mean	0.88	1.00

4. Discussion

4.1. Comparison with Previous Studies

The accuracy validation results of the urban built-up area extraction in this study indicate relatively robust outcomes with better precision compared to those of Wei et al. [22] and Xie et al. [54]. In contrast to Wei et al. [22] and Xie et al. [54], who solely employed DMSP-OLS night-time light data to confirm urban land information, this study achieved a more accurate and longer temporal sequence of the urban extent by utilizing the spatiotemporal normalized threshold method through PIFs in conjunction with NPP-VIIRS night-time light data. Zheng et al.’s research identified the highest urban expansion rates in Guangzhou and Foshan during 2012–2018 [20], aligning closely with this study’s findings for urban expansion rates in Guangzhou and Foshan during 2010–2020.

Differing from previous studies that primarily analyzed the spatiotemporal evolution pattern of urban expansion, this research not only extracted urban built-up areas based on night-time light data and Landsat imagery but also localized the SDG 11.3.1 indicator and forecasted the sustainable urbanization level within the economic belt for the 2020–2030 period under the SSP1 scenario. Currently, the differences in the calculated urban built-up area from this research and Jiang et al.’s application of a logistic regression model within feasible SSP scenarios are relatively minor [63].

4.2. Limitations and Uncertainties

The expansion of cities and the achievement of SDG11.3.1 involve various factors, including the geographical environment and policy regulations at the regional level. Therefore, this study faces certain limitations and challenges, including technical constraints related to data acquisition, as well as uncertainties in future urban expansion, and the imbalance of urban development. Further research can be conducted to address these issues.

The most significant uncertainty associated with using night-time light data lies in the relatively low brightness and wide dynamic range of night-time scenes compared to daytime remote sensing imagery [64]. Consequently, studying urban development activities over a long time series poses considerable challenges. In the process of predicting urban built-up areas, this study encountered issues of missing historical statistical data for certain years in some statistical yearbooks. Moreover, the prediction of urban expansion was carried out just using a sigmoid regression model without employing other predictive models like panel data regression models, cellular automaton modeling, etc., potentially limiting the comparison and analysis of different model predictions. To comprehensively investigate urban expansion and monitor changes in SDG11.3.1, efforts will be made to address these limitations and explore advanced models and data analysis methods.

The uncertainty of urban expansion encompasses various aspects, including the direction, scale, and pace of urban development, as well as its impacts on the surrounding environment and society. Additionally, it involves uncertainties in policy formulation and urban planning processes, along with potential uncertainties arising from conflicts and competition among different stakeholders. The imbalance in urban expansion can be attributed to various factors, including uneven resource allocation, disparities in economic development, and inconsistencies in policy formulation. These factors can lead to certain cities experiencing excessive expansion while others lag behind. For example, in our study, we observed relatively high rates of urban expansion in cities like Guangzhou and Foshan, while some other cities exhibited comparatively lower expansion rates. This discrepancy may be attributed to disparities in regional economic development and variations in government policies. In our future research, we intend to delve deeper into the fundamental reasons behind these imbalances to provide better guidance for policy formulation.

Furthermore, the incompatibility between urban expansion and the Sustainable Development Goals requires further investigation. Urban expansion can result in issues such as the overexploitation of land resources, environmental pollution, and social inequities, which run counter to the objectives of sustainable development. Future development necessitates more policies and planning to ensure the alignment of urban development with the Sustainable Development Goals. While our study serves as a starting point, further research is needed to gain a more in-depth understanding of the potential impacts of urban expansion on sustainable development and how to address these issues.

4.3. Policy Implications and Future Research Directions

The progress in SDG 11.3.1 plays a crucial role in shaping regional policies. The essence of this goal is to ensure inclusivity, safety, resilience, and sustainability in urban and human settlement areas. By delving into data related to urban expansion, resource utilization, and environmental impacts, we can gain a more comprehensive understanding of current urban expansion trends, thus providing stronger support for the development of corresponding policies in urban planning and sustainable growth. For instance, rapid urban expansion can lead to the overexploitation of resources and environmental degradation, and we can address these issues by restricting land development or enhancing environmental standards. We can offer data support to policymakers to assist them in better steering the future of urban development.

The ethical dimension within urbanization and sustainable development is of paramount importance [65]. Swift urbanization may exacerbate issues of social inequality due to an uneven distribution of resources and opportunities, potentially contradicting one of the core principles of sustainable development: inclusivity. Future research needs to thoroughly consider this aspect and ensure that the urbanization process does not further exacerbate inequality. Moreover, urban expansion may come hand in hand with environmental degradation, posing threats to ecosystem health. In urbanization and sustainable development policies, environmental protection and the maintenance of social equity are equally vital. Hence, future research directions should emphasize these ethical concerns and provide

recommendations to ensure that the urbanization process has a positive impact on all members of society and ecosystems alike.

5. Conclusions

This study used the DMSP-OLS and NPP-VIIRS night-time light data combined with high-resolution Landsat remote sensing images to extract the urban built-up areas from the Pearl River–West River Economic Belt from 2000 to 2020. Then, the spatiotemporal evolution patterns of urban expansion were analyzed. The present progress toward SDG 11.3.1 was evaluated in the current context of rapid urbanization. Finally, based on the SSP1 scenario, the study made a scientific prediction about whether the Economic Belt could achieve SDG11.3.1 by 2030. The key findings and main conclusions are as follows:

The spatiotemporal normalized threshold method of PIFs is reliable in the study area. The extracted urban area was proven to be robust with an average OA of greater than 97% and an average G-mean of greater than 82%. This indicates that the extracted results can accurately reflect the actual development of urban built-up areas within the economic belt.

From 2000 to 2020, the overall spatial and temporal patterns of urbanization across the entire Pearl River–Xijiang economic belt exhibited a significant expansion trend. However, the expansion and development among cities were uneven, resulting in evident spatiotemporal disparities in the urban built-up area expansion process within the study area.

The urban development of the whole study area was unbalanced as the urban expansion rate was lower than the population growth rate (LCRPGR = 0.33) from 2008 to 2020 but was still moving in a balanced and efficient direction. However, looking ahead to the period from 2020 to 2030, the average LCRPGR for the entire economic belt shows a significant upward trend, approaching the ideal state of sustainable development (LCRPGR \approx 1). This indicates a favorable trajectory towards achieving SDG 11.3.1 in the forthcoming decade.

Our study found an important turning point in the pattern of urban sustainable development, indicating that urban expansion and population dynamics may be harmoniously unified in the future. This transition has profound implications for guiding future urban planning and policy-making to promote balanced and sustainable urban growth. It contributes to facilitating more equitable and sustainable urban development to better meet the demands of future urbanization. Additionally, these research findings offer new research pathways for exploring the dynamics of urbanization and its consistency with broader sustainable development goals.

Author Contributions: Conceptualization, S.L.; data curation, Y.Y.; formal analysis, Y.Y.; funding acquisition, Y.Y.; investigation, B.H.; methodology, S.L. and Y.Y.; resources, B.H.; supervision, Y.Y.; visualization, S.L. and Y.Y.; writing the original draft, S.L.; writing—review and editing, Y.Y.; validation, B.H. All authors have read and agreed to the published version of the manuscript.

Funding: This research was funded by the Guangxi Science and Technology Plan Project (NO. AD20238059); and the National Natural Science Foundation of China (NO. 42061063).

Data Availability Statement: The data presented in this study are available on request from the corresponding author.

Acknowledgments: The authors wish to thank the academic editor and three anonymous referees for their very professional reviews and quite useful suggestions, which greatly helped us to improve the original version of this paper.

Conflicts of Interest: The authors declare no conflict of interest.

References

1. Cohen, B. Urbanization in developing countries: Current trends, future projections, and key challenges for sustainability. *Technol. Soc.* **2006**, *28*, 63–80. [[CrossRef](#)]
2. Habitat, U. *World Cities Report 2022: Envisaging the Future of Cities*; United Nations Human Settlements Programme: Nairobi, Kenya, 2022; pp. 41–44.

3. Wei, G.; Bi, M.; Liu, X.; Zhang, Z.; He, B.J. Investigating the impact of multi-dimensional urbanization and FDI on carbon emissions in the belt and road initiative region: Direct and spillover effects. *J. Clean. Prod.* **2023**, *384*, 135608. [[CrossRef](#)]
4. Wang, L.; Li, C.; Ying, Q.; Cheng, X.; Wang, X.; Li, X.; Gong, P. China's urban expansion from 1990 to 2010 determined with satellite remote sensing. *Chin. Sci. Bull.* **2012**, *57*, 2802–2812. [[CrossRef](#)]
5. Chen, M.; Liu, W.; Lu, D. Challenges and the way forward in China's new-type urbanization. *Land Use Policy* **2016**, *55*, 334–339. [[CrossRef](#)]
6. Wei, G.; He, B.J.; Sun, P.; Liu, Y.; Li, R.; Ouyang, X.; Li, S. Evolutionary trends of urban expansion and its sustainable development: Evidence from 80 representative cities in the belt and road initiative region. *Cities* **2023**, *138*, 104353. [[CrossRef](#)]
7. Wang, Y.; Huang, C.; Feng, Y.; Zhao, M.; Gu, J. Using earth observation for monitoring SDG 11.3. 1-ratio of land consumption rate to population growth rate in Mainland China. *Remote Sens.* **2020**, *12*, 357. [[CrossRef](#)]
8. Borana, S.L.; Yadav, S.K. Chapter 10—Urban land-use susceptibility and sustainability—Case study. In *Water, Land, and Forest Susceptibility and Sustainability*; Academic Press: Cambridge, MA, USA, 2023; Volume 2, pp. 261–286.
9. Aslam, R.W.; Shu, H.; Yaseen, A. Monitoring the population change and urban growth of four major Pakistan cities through spatial analysis of open source data. *Ann. GIS* **2023**, 1–13. [[CrossRef](#)]
10. Resolution, G.A. Transforming our World: The 2030 Agenda for Sustainable Development. UN Doc. A/RES/70/1, 25 September 2015.
11. Habitat, U.; Women, U. *SDG Goal 11 Monitoring Framework: A guide to Assist National and Local Governments to Monitor and Report on SDG Goal 11 Indicators*; Un Habitat: Nairobi, Kenya, 2016.
12. Estoque, R.C.; Ooba, M.; Togawa, T.; Hijioka, Y.; Murayama, Y. Monitoring global land-use efficiency in the context of the UN 2030 Agenda for Sustainable Development. *Habitat Int.* **2021**, *115*, 102403. [[CrossRef](#)]
13. Zhou, M.; Lu, L.; Guo, H.; Weng, Q.; Cao, S.; Zhang, S.; Li, Q. Urban sprawl and changes in land-use efficiency in the Beijing–Tianjin–Hebei region, China from 2000 to 2020: A spatiotemporal analysis using earth observation data. *Remote Sens.* **2021**, *13*, 2850. [[CrossRef](#)]
14. Gao, K.; Yang, X.; Wang, Z.; Zhang, H.; Huang, C.; Zeng, X. Spatial sustainable development assessment using fusing multisource data from the perspective of production-Living-Ecological space division: A case of greater bay area, China. *Remote Sens.* **2022**, *14*, 2772. [[CrossRef](#)]
15. Lee, C.A.; Gasster, S.D.; Plaza, A.; Chang, C.I.; Huang, B. Recent developments in high performance computing for remote sensing: A review. *IEEE J. Sel. Top. Appl. Earth Obs. Remote Sens.* **2011**, *4*, 508–527. [[CrossRef](#)]
16. Shao, Z.; Liu, C. The integrated use of DMSP-OLS nighttime light and MODIS data for monitoring large-scale impervious surface dynamics: A case study in the Yangtze River Delta. *Remote Sens.* **2014**, *6*, 9359–9378. [[CrossRef](#)]
17. Toure, S.I.; Stow, D.A.; Shih, H.C.; Weeks, J.; Lopez-Carr, D. Land cover and land use change analysis using multi-spatial resolution data and object-based image analysis. *Remote Sens. Environ.* **2018**, *210*, 259–268. [[CrossRef](#)]
18. Liu, Z.; He, C.; Zhang, Q.; Huang, Q.; Yang, Y. Extracting the dynamics of urban expansion in China using DMSP-OLS nighttime light data from 1992 to 2008. *Landsc. Urban Plan.* **2012**, *106*, 62–72. [[CrossRef](#)]
19. Lu, D.; Li, G.; Kuang, W.; Moran, E. Methods to extract impervious surface areas from satellite images. *Int. J. Digit. Earth* **2014**, *7*, 93–112. [[CrossRef](#)]
20. Zheng, Y.; He, Y.; Zhou, Q.; Wang, H. Quantitative evaluation of urban expansion using NPP-VIIRS nighttime light and Landsat spectral data. *Sustain. Cities Soc.* **2022**, *76*, 103338. [[CrossRef](#)]
21. Chen, J.; Zhuo, L.; Shi, P.J.; Toshiaki, I. The study on urbanization process in China based on DMSP/OLS data: Development of a light index for urbanization level estimation. *J. Remote Sens. Beijing* **2003**, *7*, 168–175.
22. Wei, Y.; Liu, H.; Song, W.; Yu, B.; Xiu, C. Normalization of time series DMSP-OLS nighttime light images for urban growth analysis with pseudo invariant features. *Landsc. Urban Plan.* **2014**, *128*, 1–13. [[CrossRef](#)]
23. Cao, C.; De Luccia, F.J.; Xiong, X.; Wolfe, R.; Weng, F. Early on-orbit performance of the visible infrared imaging radiometer suite onboard the Suomi National Polar-Orbiting Partnership (S-NPP) satellite. *IEEE Trans. Geosci. Remote Sens.* **2013**, *52*, 1142–1156. [[CrossRef](#)]
24. Zhao, M.; Zhou, Y.; Li, X.; Cao, W.; He, C.; Yu, B.; Li, X.; Elvidge, C.D.; Cheng, W.; Zhou, C. Applications of satellite remote sensing of nighttime light observations: Advances, challenges, and perspectives. *Remote Sens.* **2019**, *11*, 1971. [[CrossRef](#)]
25. Milesi, C.; Elvidge, C.D.; Nemani, R.R.; Running, S.W. Assessing the impact of urban land development on net primary productivity in the southeastern United States. *Remote Sens. Environ.* **2003**, *86*, 401–410. [[CrossRef](#)]
26. Muthukrishnan, R.; Radha, M. Edge detection techniques for image segmentation. *Int. J. Comput. Sci. Inf. Technol.* **2011**, *3*, 259. [[CrossRef](#)]
27. Su, Y.; Chen, X.; Wang, C.; Zhang, H.; Liao, J.; Ye, Y.; Wang, C. A new method for extracting built-up urban areas using DMSP-OLS nighttime stable lights: A case study in the Pearl River Delta, southern China. *GIScience Remote Sens.* **2015**, *52*, 218–238. [[CrossRef](#)]
28. Quarmbay, N.; Cushnie, J. Monitoring urban land cover changes at the urban fringe from SPOT HRV imagery in south-east England. *Int. J. Remote Sens.* **1989**, *10*, 953–963. [[CrossRef](#)]
29. Wu, K.; Wang, X. Aligning pixel values of DMSP and VIIRS nighttime light images to evaluate urban dynamics. *Remote Sens.* **2019**, *11*, 1463. [[CrossRef](#)]
30. Allen, C.; Metternicht, G.; Wiedmann, T. Initial progress in implementing the Sustainable Development Goals (SDGs): A review of evidence from countries. *Sustain. Sci.* **2018**, *13*, 1453–1467. [[CrossRef](#)]

31. Lee, K.H.; Noh, J.; Khim, J.S. The Blue Economy and the United Nations' sustainable development goals: Challenges and opportunities. *Environ. Int.* **2020**, *137*, 105528. [CrossRef]
32. Szetey, K.; Moallemi, E.A.; Ashton, E.; Butcher, M.; Sprunt, B.; Bryan, B.A. Co-creating local socioeconomic pathways for achieving the sustainable development goals. *Sustain. Sci.* **2021**, *16*, 1251–1268. [CrossRef]
33. Karimi, F.; Sultana, S.; Babakan, A.S.; Suthaharan, S. An enhanced support vector machine model for urban expansion prediction. *Comput. Environ. Urban Syst.* **2019**, *75*, 61–75. [CrossRef]
34. Chen, G.; Li, X.; Liu, X.; Chen, Y.; Liang, X.; Leng, J.; Xu, X.; Liao, W.; Qiu, Y.; Wu, Q.; et al. Global projections of future urban land expansion under shared socioeconomic pathways. *Nat. Commun.* **2020**, *11*, 537. [CrossRef]
35. O'Neill, B.C.; Kriegler, E.; Riahi, K.; Ebi, K.L.; Hallegatte, S.; Carter, T.R.; Mathur, R.; Van Vuuren, D.P. A new scenario framework for climate change research: The concept of shared socioeconomic pathways. *Clim. Chang.* **2014**, *122*, 387–400. [CrossRef]
36. Van Vuuren, D.P.; Stehfest, E.; Gernaat, D.E.; Doelman, J.C.; Van den Berg, M.; Harmsen, M.; de Boer, H.S.; Bouwman, L.F.; Daioglou, V.; Edelenbosch, O.Y.; et al. Energy, land-use and greenhouse gas emissions trajectories under a green growth paradigm. *562 Glob. Environ. Chang.* **2017**, *42*, 237–250. [CrossRef]
37. Clarke, K.C.; Gaydos, L.J. Loose-coupling a cellular automaton model and GIS: Long-term urban growth prediction for San Francisco and Washington/Baltimore. *Int. J. Geogr. Inf. Sci.* **1998**, *12*, 699–714. [CrossRef] [PubMed]
38. Li, X.; Yeh, A.G.O. Modelling sustainable urban development by the integration of constrained cellular automata and GIS. *Int. J. Geogr. Inf. Sci.* **2000**, *14*, 131–152. [CrossRef]
39. Tripathy, P.; Kumar, A. Monitoring and modeling spatio-temporal urban growth of Delhi using Cellular Automata and geoinformatics. *Cities* **2019**, *90*, 52–63. [CrossRef]
40. Pijanowski, B.C.; Brown, D.G.; Shellito, B.A.; Manik, G.A. Using neural networks and GIS to forecast land use changes: A land transformation model. *Comput. Environ. Urban Syst.* **2002**, *26*, 553–575. [CrossRef]
41. Mohammady, S.; Delavar, M.R. Urban sprawl assessment and modeling using landsat images and GIS. *Model. Earth Syst. Environ.* **2016**, *2*, 155. [CrossRef]
42. Gharaibeh, A.; Shaamala, A.; Obeidat, R.; Al-Kofahi, S. Improving land-use change modeling by integrating ANN with Cellular Automata-Markov Chain model. *Heliyon* **2020**, *6*. [CrossRef]
43. d'Aquino, P.; August, P.; Balmann, A.; Berger, T.; Bousquet, F.; Brondizio, E.; Brown, D.G.; Couclelis, H.; Deadman, P.; Goodchild, M.F.; et al. Agent-based models of land-use and land-cover change. In Proceedings of the International Workshop, Yufuin, Japan, 11–14 September 2002; Volume 577, pp. 4–7.
44. Li, J.; Oyana, T.J.; Mukwaya, P.I. An examination of historical and future land use changes in Uganda using change detection methods and agent-based modeling. *Afr. Geogr. Rev.* **2016**, *35*, 247–271.
45. Kaviari, F.; Mesgari, M.S.; Seidi, E.; Motieyan, H. Simulation of urban growth using agent-based modeling and game theory with different temporal resolutions. *Cities* **2019**, *95*, 102387. [CrossRef]
46. Hu, Z.; Lo, C. Modeling urban growth in Atlanta using logistic regression. *Comput. Environ. Urban Syst.* **2007**, *31*, 667–688. [CrossRef]
47. Angel, S.; Parent, J.; Civco, D.L.; Blei, A.; Potere, D. The dimensions of global urban expansion: Estimates and projections for all countries, 2000–2050. *Prog. Plan.* **2011**, *75*, 53–107. [CrossRef]
48. Arsanjani, J.J.; Helbich, M.; Kainz, W.; Boloorani, A.D. Integration of logistic regression, Markov chain and cellular automata models to simulate urban expansion. *Int. J. Appl. Earth Obs. Geoinf.* **2013**, *21*, 265–275. [CrossRef]
49. Zhao, Y.S.F. Spatial and temporal evolutionary characteristics of ecosystem service values under differential economic growth—A case study of the Pearl River-Xijiang Economic Belt. *J. Nat. Resour.* **2022**, *37*, 1782–1798.
50. National Development and Reform Commission. Pearl River (Guan Dong)—Xi Jiang River Economic Belt Development Plan. Available online: <http://www.gov.cn/foot/site1/20140801/95841406863847398.pdf> (accessed on 24 August 2021).
51. Chen, Y.; Li, X.; Huang, K.; Luo, M.; Gao, M. High-resolution gridded population projections for China under the shared socioeconomic pathways. *Earth's Future* **2020**, *8*, e2020EF001491. [CrossRef]
52. Wang, T.; Sun, F. Global gridded GDP data set consistent with the shared socioeconomic pathways. *Sci. Data* **2022**, *9*, 221. [CrossRef]
53. Zhang, Q.; Seto, K.C. Mapping urbanization dynamics at regional and global scales using multi-temporal DMSP/OLS nighttime light data. *Remote Sens. Environ.* **2011**, *115*, 2320–2329. [CrossRef]
54. Xie, Y.; Weng, Q. Updating urban extents with nighttime light imagery by using an object-based thresholding method. *Remote Sens. Environ.* **2016**, *187*, 1–13. [CrossRef]
55. Chen, L.; Li, X.; Yao, Y.; Chen, D.S. Analysis on the Impact of Population Agglomeration on Urban Economic Growth in China. *Acta Geogr. Sin.* **2018**, *73*, 1107–1120.
56. Henderson, M.; Yeh, E.T.; Gong, P.; Elvidge, C.; Baugh, K. Validation of urban boundaries derived from global night-time satellite imagery. *Int. J. Remote Sens.* **2003**, *24*, 595–609. [CrossRef]
57. Kubat, M.; Holte, R.C.; Matwin, S. Machine learning for the detection of oil spills in satellite radar images. *Mach. Learn.* **1998**, *30*, 195–215. [CrossRef]
58. Wang, X.; Bao, Y. Study on the methods of land use dynamic change research. *Prog. Geogr.* **1999**, *18*, 81–87.
59. Wu, W.; Zhao, S.; Zhu, C.; Jiang, J. A comparative study of urban expansion in Beijing, Tianjin and Shijiazhuang over the past three decades. *Landsc. Urban Plan.* **2015**, *134*, 93–106. [CrossRef]

60. United Nations Human Settlements Program. Module 3: Land Consumption Rate. Available online: https://www.unescwa.org/sites/www.unescwa.org/files/u593/Module3land_consumption_edite586d_23-03-2018.pdf (accessed on 16 September 2022).
61. Calka, B.; Orych, A.; Bielecka, E.; Mozuriunaite, S. The ratio of the land consumption rate to the population growth rate: A framework for the achievement of the spatiotemporal pattern in Poland and Lithuania. *Remote Sens.* **2022**, *14*, 1074. [[CrossRef](#)]
62. Li, X.; Zhou, Y.; Eom, J.; Yu, S.; Asrar, G.R. Projecting global urban area growth through 2100 based on historical time series data and future shared socioeconomic pathways. *Earth's Future* **2019**, *7*, 351–362. [[CrossRef](#)]
63. Jiang, H.; Guo, H.; Sun, Z.; Xing, Q.; Zhang, H.; Ma, Y.; Li, S. Projections of urban built-up area expansion and urbanization sustainability in China's cities through 2030. *J. Clean. Prod.* **2022**, *367*, 133086. [[CrossRef](#)]
64. Zheng, Y.; Tang, L.; Wang, H. An improved approach for monitoring urban built-up areas by combining NPP-VIIRS nighttime light, NDVI, NDWI, and NDBI. *J. Clean. Prod.* **2021**, *328*, 129488. [[CrossRef](#)]
65. De Souza, M.L. Urban development on the basis of autonomy: A politico-philosophical and ethical framework for urban planning and management. *Ethics Place Environ.* **2000**, *3*, 187–201. [[CrossRef](#)]

Disclaimer/Publisher's Note: The statements, opinions and data contained in all publications are solely those of the individual author(s) and contributor(s) and not of MDPI and/or the editor(s). MDPI and/or the editor(s) disclaim responsibility for any injury to people or property resulting from any ideas, methods, instructions or products referred to in the content.